Peer-reviewed version available at Sensors 2018, 18, 3927; doi:10.3390/s18113927

Novel competitive fluorescence sensing platform for L-carnitine based on cationic pillar[5]arene modified gold nanoparticles

Xiaoping Tan [a,*], Yang Yang [a], Shasha Luo [a], Zhong Zhang [a], Wenjie Zeng [a], Tingying Zhang [a], Fawu Su [b,*], Linzong Zhou [c,*]

[a] Key Lab of Inorganic Special Functional Materials, Chongqing Municipal Education Commission, School of Chemistry and Chemical Engineering, Yangtze Normal University, Fuling 408100, Chongqing, China

[b] State Key Laboratory for Conservation and Utilization of Bio-Resources in Yunnan, Yunnan Agricultural University, Kunming 650224, Yunnan, China

[c] School of geographical science and tourism management, Chuxiong Normal University, Chuxiong 675000, Yunnan, China

***Corresponding Author**

E-mail: xptan@yznu.cn (X. Tan); sufaw@ynau.edu.cn (F. Su); zhonglinzong@163.com

Peer-reviewed version available at Sensors 2018, 18, 3927; doi:10.3390/s18113927

Abstract: A supramolecular host-guest interaction and sensing between cationic pillar[5]arenes (CP5) and L-carnitine were developed by the competitive host-guest recognition for the first time. The fluorescence sensing platform was constructed by CP5 functionalized Au nanoparticles (PP5@Au-NPs) as receptor and probe (rhodamine 123, R123), which shown a high sensitivity and selectivity to L-carnitine detection. Due to the property of the negative charge and molecular size of L-carnitine, it can be highly captured by the CP5 via electrostatic interactions and hydrophobic interactions. The mechanism of host-guest between PP5 and L-carnitine was studied by ^{1}H NMR and molecular docking, which indicated more affinity binding force of PP5 with L-carnitine. Therefore, a selective and sensitive fluorescent method was developed. It has a linear response of 0.1−2.0 and 2.0−25.0 μM and a detection limit of 0.067 μM (S/N=3) for L-carnitine. The fluorescent sensing platform was also used to detect L-carnitine in human serum and milk samples, which provided potential applications of detection drugs of abuse, and had path for guarding a serious food safety issues.

Keywords: cationic pillar[5]arenes, host–guest recognition, Au nanoparticles, L-carnitine

1. Introduction

Gold nanoparticles (Au-NPs) have the characteristics of facile synthesis, high chemical stability and easy surface functionalization, which have attracted the great interest of researchers in the fields of nanotechnology and nanomaterials because of their importance in biomedicine [1], sensing [2], catalysis [3], nanoelectronics [4,5], et al. For this reason, many novel hybrid nanomaterials are designed to synthesize Au-NPs with morpholog, size, and composition control [6,7]. The interactions of nanoparticles with surface ligands is also a key aspect for many applications. For example, appropriate surface modification of the nanoparticles can improve their sensor potential.

Macrocyclic arenes play an important role in the field of supramolecular chemistry [8-10]. After crown ethers, calixarenes, cyclodextrins, and cucurbiturils [11,12], pillar[n]arenes are the fifth class of macrocyclic host molecules, and they were first reported by Ogoshi [13]. Pillar[n]arenes mainly consist of pillar[5]arenes and pillar[6]arenes, which are linked by methylene bridges at their *para*-positions to form a unique rigid pillar architecture. Pillar[n]arenes are important players in supramolecular chemistry due to their easy synthesis, unique pillar shape, symmetrical structure, excellent host-guest properties, and natural supramolecular assembly characteristics. They have numerous potential applications in host-guest chemistry, hybrid nanomaterials, and biomedical material [14-18]. At present, much research has focused on the synthesis and of pillar[n]arenes, their host−guest chemistry and supramolecular self-assembly [19,20]. The combination of metal nanoparticles and supramolecular macrocyclic compounds could produce strong synergistic effects, and improve the properties of nanoparticles, where host-guest chemistry could play an important role [21]. However, the conjugation of pillar[n]arenes with Au-NPs and the application of the resulting hybrid nanomaterials remain rarely reported [22].

Stabilizing ligands possessing carboxyl (−COOH), sulfhydryl (−SH) and amine ($-NH_2$) groups are crucial to the synthesis and stabilization of Au-NPs [23-25]. Yang et al produced a new carboxylatopillar[5]arene-modified Au-NPs with good dispersion and narrow size distributions in aqueous solution, the supramolecular self-assembly of CP[5]A@Au-NPs is very useful for sensor and detection of the paraquat [26]. Huang et al first reported a novel type of amphiphilic Au-NPs with bilayers of an amphiphilic pillar[5]arene modified on their surfaces, which can be used in the fabrication of self-assembled composite microtubes (SCMTs), and these SCMTs are excellent catalysts [27]. Pastoriza-Santos et al prepared an ammonium pillar[5]arene-stabilized Au-NPs with shape and size control by using seeded growth. The ammonium pillar[5]arene-stabilized Au-NPs were applied to detect 2-naphthoic acid and polycyclic aromatic hydrocarbons [28]. Recently, Yang et al fabricated the green synthesis of hydroxylatopillar[5]arene-modified Au-NPs (HP5@Au-NPs). The

HP5@Au-NPs can self-assemble into multiple well-defined architectures, and employ as not only scaffolds but energy acceptors for turn-on fluorescence sensor based on a competitive host−guest interaction [29]. Despite enormous development that has been achieved in self-assembly of pillar[5]arene-based Au-NPs in recent years, it still remains a great need to further develop their application of the resulting hybrid nanomaterials.

L-carnitine is also called (3R)-3-hydroxy-4-(trimethylammonio)butanoate, which is a naturally occurring substance, essential for fatty acid oxidation and energy production in the human body [30,31]. Deficiency of L-carnitine results in major energy loss and toxic accumulations of free fatty acids. Though many methods have used for detecting L-carnitine, such as chromatography [32], capillary electrophoresis [33,34], voltammetric [35], fluorescence [36-38], etc, there still remains the great challenge to find a selective sensitive tool to detect L-carnitine. Fluorescence technique as a promising method for detection of L-carnitine exhibits many advantages over other common detection techniques, such as good portability, low-cost, high sensitivity and selectivity [39].

Herein, we describe a simple and convenient “turn-off-on” fluorescent sensing platform between cationic pillar[5]arenes (CP5) and L-carnitine. The fluorescence sensing platform is constructed by CP5@Au-NPs as receptor and probe R123, which shows a high sensitivity and selectivity to detect L-carnitine. The competitive fluorescence sensing platform based on CP5@Au-NPs is illustrated in **Scheme. 1**. This method is simple, low cost, sensitive, selective, and has been applied to L-carnitine detection in human serum and milk samples.

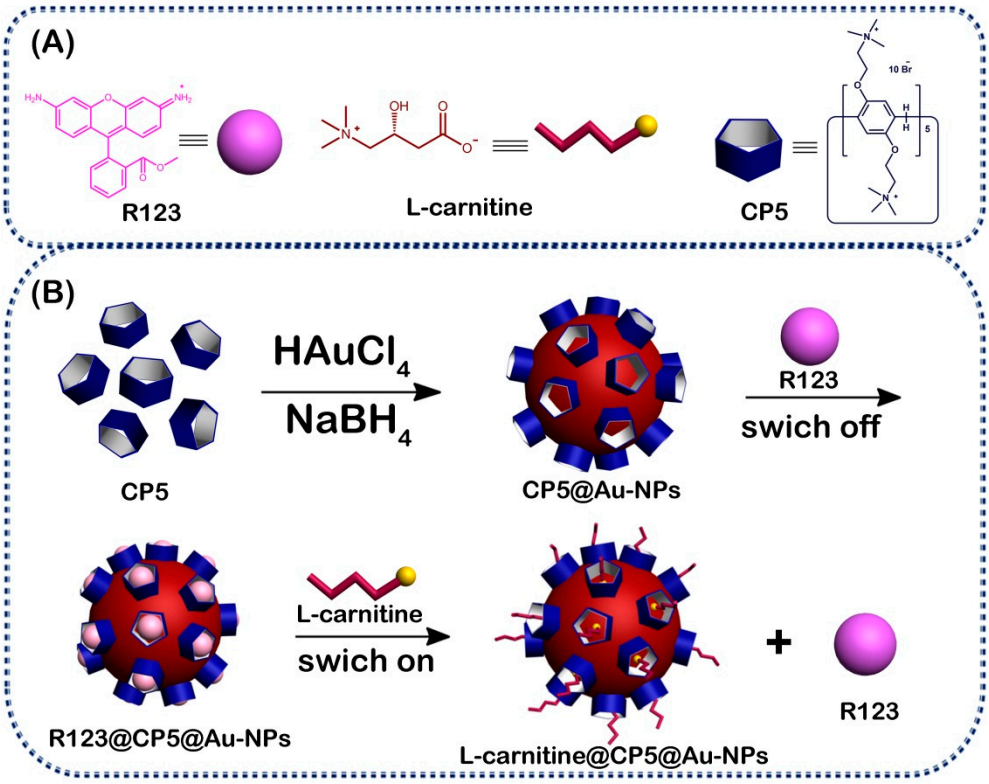

Scheme 1. The corresponding cartoon representations of R123, L-carnitine, CP5 (A), and the illustration of CP5@Au-NPs hybrid nanomaterials-based fluorescent sensing method towards L-carnitine (B).

2. Experiment section

2.1. Reagents and apparatus

$HAuCl_4$, Rhodamine 123 (R123), L-carnitine，and $NaBH_4$ were obtained from Shanghai Titan Scientific Co. Ltd. CP5 was synthesized by the literature [40,41], and the synthetic route is shown in **Scheme. 2**. The synthetic details are described in the Supporting Information (SI). Other chemicals were of analytical grade. Deionized water (DW, 18 MΩ cm) was used to prepare all of the aqueous solutions.

Preprints (www.preprints.org) | NOT PEER-REVIEWED | Posted: 24 October 2018 doi:10.20944/preprints201810.0573.v1

Peer-reviewed version available at Sensors 2018, 18, 3927; doi:10.3390/s18113927

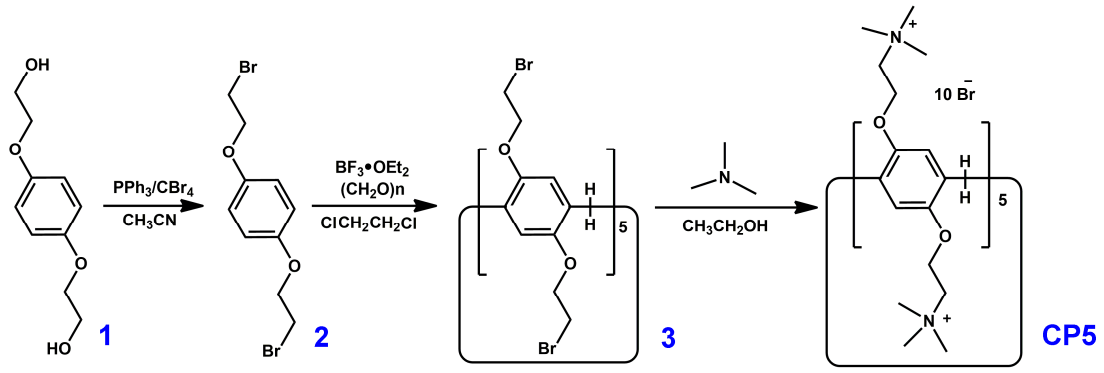

Scheme 2. The synthetic route of macrocyclic host CP5.

2.2. Apparatus and instruments

The samples were characterized by Fourier transform infrared (FTIR) spectroscopy via the SCIENTIFIC Nicolet IS10 (Massachusetts, USA) FTIR impact 410 spectrophotometer using KBr pellets at a wavelength of 4000–400 cm^{-1}. The X-ray photoelectron spectroscopy (XPS) was performed on an ESCALAB-MKII spectrometer (VG Co., United Kingdom) with Al Ka X-ray radiation as the X-ray source for excitation. EDS was carried out in the JEM 2100 transmission electron microscopy (TEM, Japan) equipped with an energy dispersive X-ray spectrometry. The zeta potential of the sample was measured with a Malvern Zetasizer Nano series. Fluorescent titrimetric experiments were performed on a Hitachi F-4500 spectrophotometer (Tokyo, Japan). ^{1}H NMR and ^{13}C NMR spectra were recorded on a Bruker Avance DMX-400 spectrometer at 400 MHz and 500 MHz.

2.3. Synthesis of the CP5@Au-NPs

The CP5@Au-NPs composite was obtained according to a similar work [22,28]. The CP5@Au-NPs were synthesized by reducing $HAuCl_4$ in presence of CP5. In a typical synthetic procedure, an aqueous solution of CP5 (100 μM, 2000 μL) and an aqueous solution of $HAuCl_4$ (10 mM, 200 μL) were added to DW (10 mL), then the fresh aqueous solution of $NaBH_4$ (40 μL, 0.1M) was added into the mixture under vigorous stirring. And the solution got wine red, which indicated that cationic

pillar[5]arene-modified Au nanoparticles were prepared.

2.4. Experiments for titration L-carnitine

Aqueous solutions of R123 (200 μM), L-carnitine (400 μM), and CP5@Au-NPs (1.0 mg mL^{-1}) were prepared. A final concentration of 2 μM R123 was also obtained via dilution. By gradually addition of CP5@Au-NPs dispersion to the R123 solution, and the fluorescence of the R123 was gradually quenched. The competitive displacement experiments were performed as follows: the L-carnitine solution was gradually added to a complex of R123-bound CP5@Au-NPs to displace the R123 molecule from the cavity of CP5 by L-carnitine. The fluorescence signal was measured and recorded after the combined solution was mixed by vortexing for 3 min.

3. Results and discussion

3.1. Characterization of the CP5@Au-NPs

Firstly, according to the surface plasmon resonance (SPR) of Au-NPs at ~520 nm, the UV-vis absorption of different concentrations of [CP5]/[$HAuCl_4$] were obtained and shown in **Fig. S7**. Upon increasing value of [CP5]/[$HAuCl_4$] from 0.05 to 1, the SPR peak maximum almost not charged, which suggested that the excess CP5 had little influence to the sizes of Au-NPs. The synthesized CP5@Au-NPs were win red (**Fig. S8**) and the UV-vis spectroscopy absorption shown at ~520 nm (**Fig. 1A**), which demonstrated that CP5 stabilized and modified Au-NPs were successfully synthesized. We further studied the morphology features of CP5@Au-NPs by the TEM. As shown in **Fig. 2B**, CP5 modified Au nanoparticles (CP5@Au-NPs) with spherical structure were successfully prepared and the size of CP5@Au-NPs was greatly uniform and homogeneous dispersion, which was ascribed to the outstanding size regulating and stabilized effect of CP5 by the coordination between Au-NPs and quaternary ammonium salt groups of CP5. The high resolution transmission electron

Preprints (www.preprints.org) | NOT PEER-REVIEWED | Posted: 24 October 2018 doi:10.20944/preprints201810.0573.v1

Peer-reviewed version available at Sensors 2018, 18, 3927; doi:10.3390/s18113927

microscopy (HRTEM) images of CP5@Au-NPs (**Figs. 1C** and **1D**) shown that the corresponding CP5@Au-NPs diameter and crystal lattice spacing were approximately 7 nm and 0.285 nm, respectively. The small size and homogeneous dispersion of CP5@Au-NPs lead to the high catalytic activity and fluorescence quenching property, which indicate that CP5@Au-NPs have potential application in sensing and catalysis.

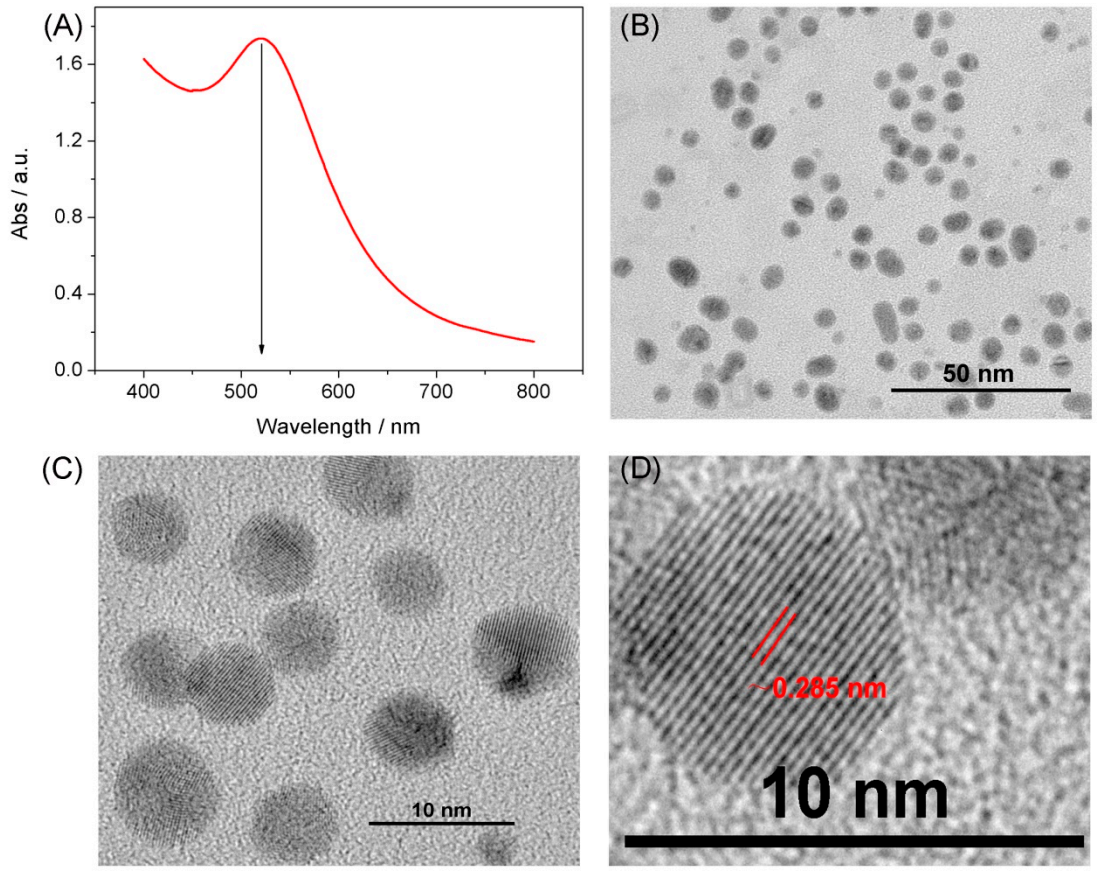

Figure 1. UV-vis adsorption spectrum of CP5@Au-NPs (A); TEM image of CP5@Au-NPs (B); HRTEM images of CP5@Au-NPs (C and D).

The CP5@Au-NPs were characterized by zeta potential and results shown in **Fig. 2A** and **2B**. In general, the ξ-potential values of Au-NPs is almost zero because the surface of Au-NPs has no charge. Therefore, different charge groups modified Au-NPs will lead to different ξ-potential values. By comparing the zeta potential value 12.5 mV of CP5 (**Fig. 2B**), the zeta potential value of CP5@Au-NPs (**Fig. 2A**) is the 35.2 mV that almost is 3 times than CP5, which suggests that CP5 successfully modifies Au-NPs to form CP5@Au-NPs. FTIR spectroscopy was used to verify if

198 macrocyclic molecule CP5 capped on the Au-NPs. From the FTIR spectroscopy of
199 CP5@Au-NPs and CP5 (**Fig. 2 C**), as compared to bare CP5, a typical absorption
200 peak at 1625, 1491, and 1407 cm^{-1} of benzene ring in CP5 and absorption peak at
201 2975 and 2846 cm^{-1} of $–CH_3$ and $–CH_2–$ in CP5 were observed in CP5@Au-NPs
202 FTIR spectroscopy, which shown that the Au-NPs were capped by CP5. We used XPS
203 for proving the presence of CP5 on surface of Au-NPs. As shown in **Fig. 2D**, for pure
204 CP5, three peaks were observed at 532.5, 402.1, and 285.1 of O 1s, N 1s, and C1s,
205 respectively. However, for the CP5@Au-NPs, a pronounced Au 4f peak was observed,
206 which further indicated that the Au-NPs had successfully been modified by CP5. As
207 shown in **Fig. 2E**, the Au $4f_{5/2}$ peak at 87.6 eV and Au $4f_{7/2}$ peak at 83.8 eV were
208 observed and the results were similar with the reported [42-44], which illustrated that
209 CP5@Au-NPs successful were obtained. The prepared CP5@Au-NPs were further
210 characterized by EDS for to investigate the elements of CP5@Au-NPs and shown in
211 **Fig. 2F**. An obvious Au element was observed at CP5@Au-NPs, which further
212 indicated that the modified processes had been taken place between CP5 and Au-NPs.
213 Therefore, above results could suggest that CP5 had successfully grafted on the
214 Au-NPs and formed the CP5@Au-NPs hybrid nanomaterias.

Preprints (www.preprints.org) | NOT PEER-REVIEWED | Posted: 24 October 2018 doi:10.20944/preprints201810.0573.v1

Peer-reviewed version available at Sensors 2018, 18, 3927; doi:10.3390/s18113927

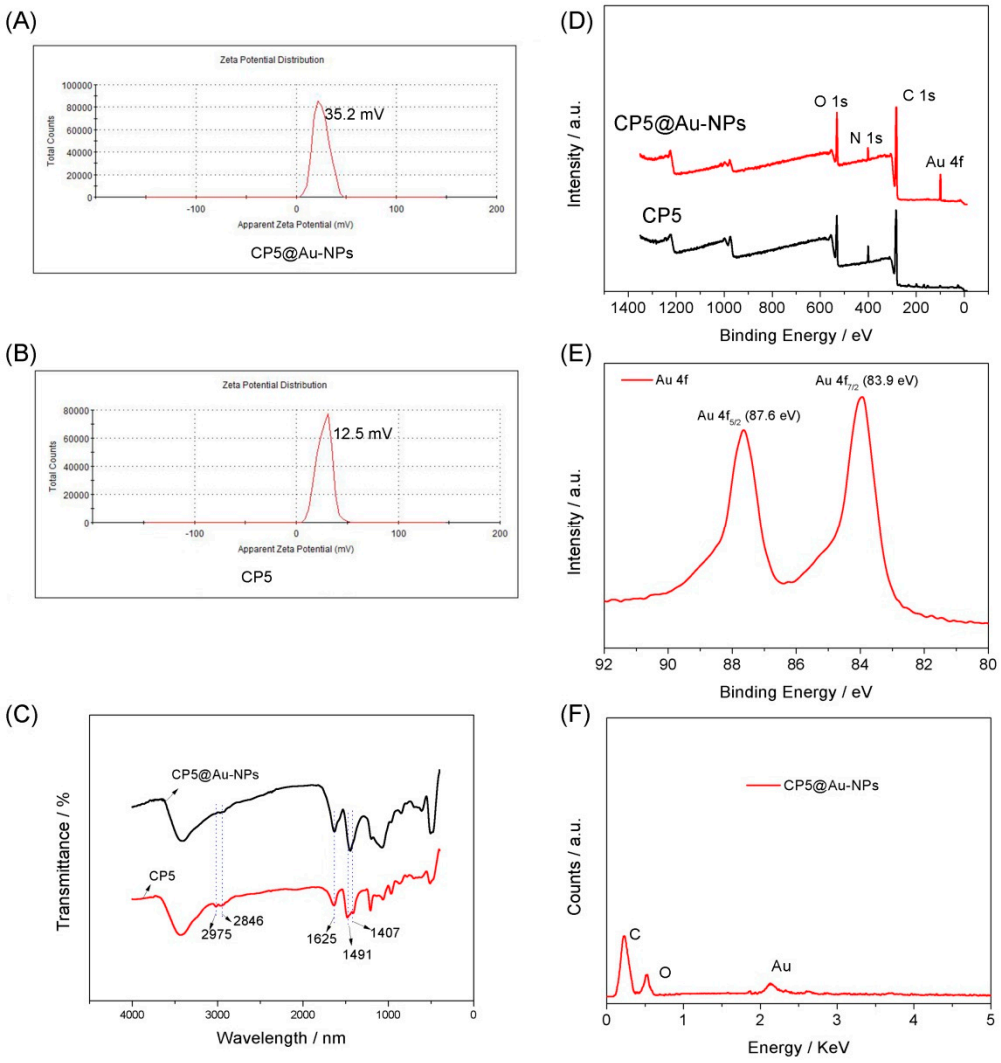

Figure 2. Zeta potentials of CP5@Au-NPs (A); Zeta potential of CP5 (B); FTIR spectra of CP5@Au-NPs and CP5 (C); XPS survey spectrum of CP5@Au-NPs and CP5 (D); high resolution XPS spectra of Au_{4f} (E); EDS spectra of CP5@Au-NPs (F).

3.2. Fluorescence spectra analysis

The study of the fluorescence quenching performance with CP5 and CP5@Au-NPs towards R123 was developed and shown in **Fig. 3A**. As we can distinctly see from **Fig. 3A** that the fluorescence intensity of R123 was quenched by CP5@Au-NPs for the reason of fluorescence resonance energy transfer between R123 and Au-NPs. The R123 was connected by CP5 to Au-NPs and the fluorescence was quenched. Therefore, the fluorescence intensity of R123 was continuously quenched

with the increasing of the CP5@Au-NPs amount and shown in **Fig. 3B**. Because of suitable structure/size, the probe R123 can enter the cavity of CP5 via the host-guest recognition, which leads to fluorescence quenching by effective energy transfer from probe to Au-NPs. **Fig. 3C** shows that the successive reversion of the fluorescence signal of R123 was observed with the successive increase of L-carnitine towards the pre-formed R123@CP5@Au-NPs inclusion complex. The fluorescence signal reversion was caused by the adding of the amount of L-carnitine, which suggested that the successful detection of L-carnitine by using this fluorescence approach. Therefore, this phenomenon can be concluded that the R123 entered into the cavity of CP5 and formed inclusion complex with CP5@Au-NPs. In addition, the R123 molecule was released from the cavity of CP5 by the addition of L-carnitine based on the competitive supramolecular recognition. Herein, a phenomenon of "turn−off−on" fluorescence process was developed. Besides, the R123 was incubated with CP5@Au-NPs to form R123@CP5@Au-NPs complexation and attached the Au-NPs, and accompanied by the phenomena of indicator fluorescence 'turn off' on account of the fluorescence resonance energy transfer (FRET) [29,45-47]. Some control experiments had been performed for confirming that observed fluorescence intensity recovery was caused by the displacement of R123 by L-carnitine from the cavity of host molecule CP5. We further researched the phenomenon of fluorescence reversion of R123 in the presence of Au-NPs. As shown in **Fig. S9A** and **S9B**, although the fluorescence quenching phenomenon obviously taken place between Au-NPs and R123, the fluorescence reversion did not occur with the addition of L-carnitine. Therefore, this processes can be concluded that dye indicator R123 firstly combined with CP5@Au-NPs and then was released from CP5@Au-NPs upon the addition of L-carnitine, which formed a fluorescence "switch off on".

Preprints (www.preprints.org) | NOT PEER-REVIEWED | Posted: 24 October 2018 doi:10.20944/preprints201810.0573.v1

Peer-reviewed version available at Sensors 2018, 18, 3927; doi:10.3390/s18113927

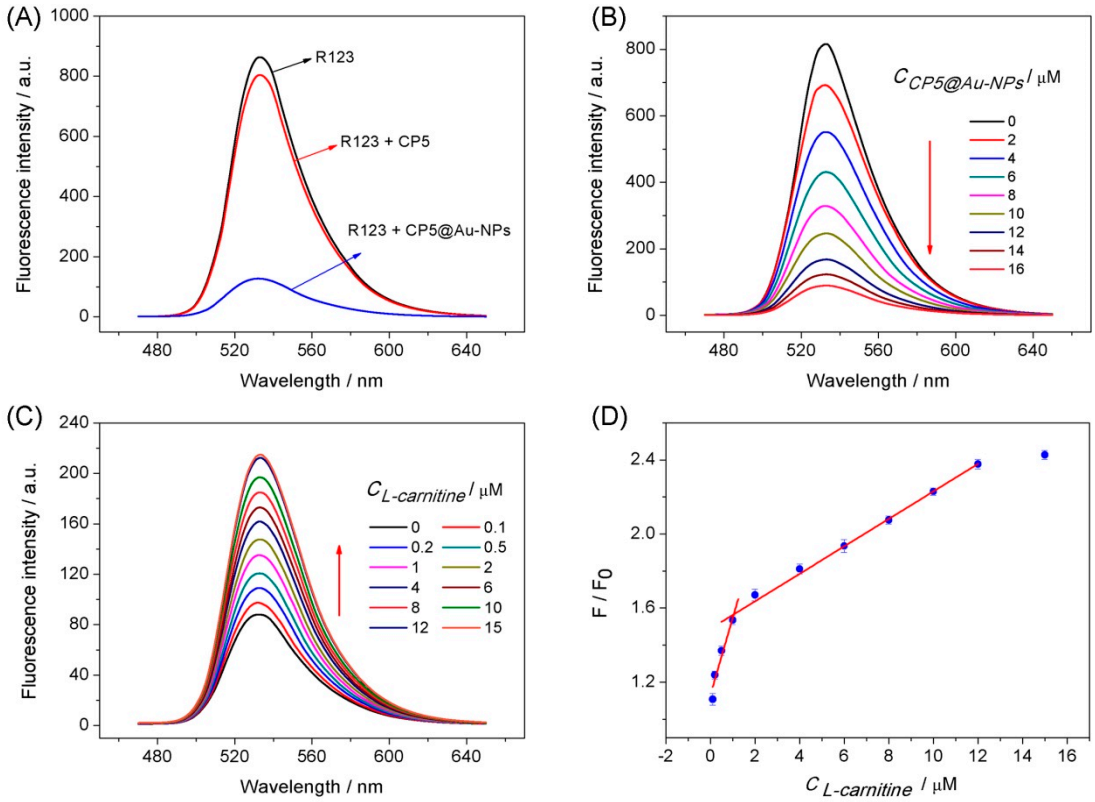

Figure 3. The fluorescence intensity of 2 μM R123 in the presence of 10 μM CP5 and 16 μg mL^{-1} CP5@Au-NPs (A). The effect of increasing concentrations of CP5@Au-NPs (concentrations ranging from 0 μg/mL to 16 μg/mL) on the fluorescence intensity of R123 dispersion (B). Fluorescence spectra of the R123@CP5@Au-NPs complexes via different concentrations of L-carnitine (C). Calibration curves of fluorescent intensity for R123@CP5@Au-NPs vs. L-carnitine concentrations (D).

Fig. 3D presents the calibration curves for the quantitative determination of L-carnitine, and the fluorescence ratio F/F_0 was proportional to the concentration of L-carnitine. The linear response ranges for L-carnitine detection were 0.1−2.0 and 2.0−25.0 μM. The detection limit was 0.067 μM (S/N=3), and the corresponding regression equations of F/F_0=0.41 C (μM) + 1.13 and F/F_0=0.07 C (μM) + 1.48 with correlation coefficients of 0.925 and 0.995 were obtained. This approach was compared to other methods for detection of L-carnitine (**Table S1**). This competitive fluorescent method showed a wider linear range, lower detection limit, and high

selectivity versus previously reported approaches. Moreover, this method is very convenient and simple for the determination of L-carnitine and has potential applications in sensing of L-carnitine in human blood and food.

3.3. The analysis of host–guest recognition

The procedure of recognition between CP5 and L-carnitine was studied by the molecular docking. The inclusion model of L-carnitine with CP5 was obtained by using the AutoDock 4.2.6 [48] and illustrated in **Figs. 4A** and **4B**. Due to the cavity size of CP5 and the molecular size of L-carnitine, thus they could recognize with 1:1 guest–host complex. As we can see from the **Fig. 4A** and **4B**, the negative charge of carboxylate in L-carnitine could form a higher capacity electrostatic interaction with positive charge groups of $-N(CH_3)_3^+$ in CP5 (**Fig. 4C**). In addition, the quaternary ammonium salt of L-carnitine could form the cation-π interaction with the five benzene rings of CP5, and the quaternary ammonium salt of L-carnitine entered the cavity of CP5 by hydrophobic interaction (**Fig. 4D**). However, it was not insufficiency to explain the recognized mechanism by molecular docking. The host-guest recognition between CP5 and L-carnitine was also studied by the ^1H NMR, and the result was shown in **Fig. 5**. It is clear that the proton Ha and Hb of L-carnitine disappeared after complexation, and the H1 and H5 of CP5 have shifted upfield, which demonstrated that the CP5 can bind L-carnitine with more affinity to release R123 and other interference. Therefore, a selective platform of detection L-carnitine by CP5@Au-NPs was obtained. Due to the negative charge of L-carnitine and positive charge of CP5, the more affinity electrostatic interaction has taken place between L-carnitine and CP5, which plays an important role in host-guest interaction [49-51]. And the guest L-carnitine can be recognized by host CP5 via the electrostatic interaction and hydrophobic interaction.

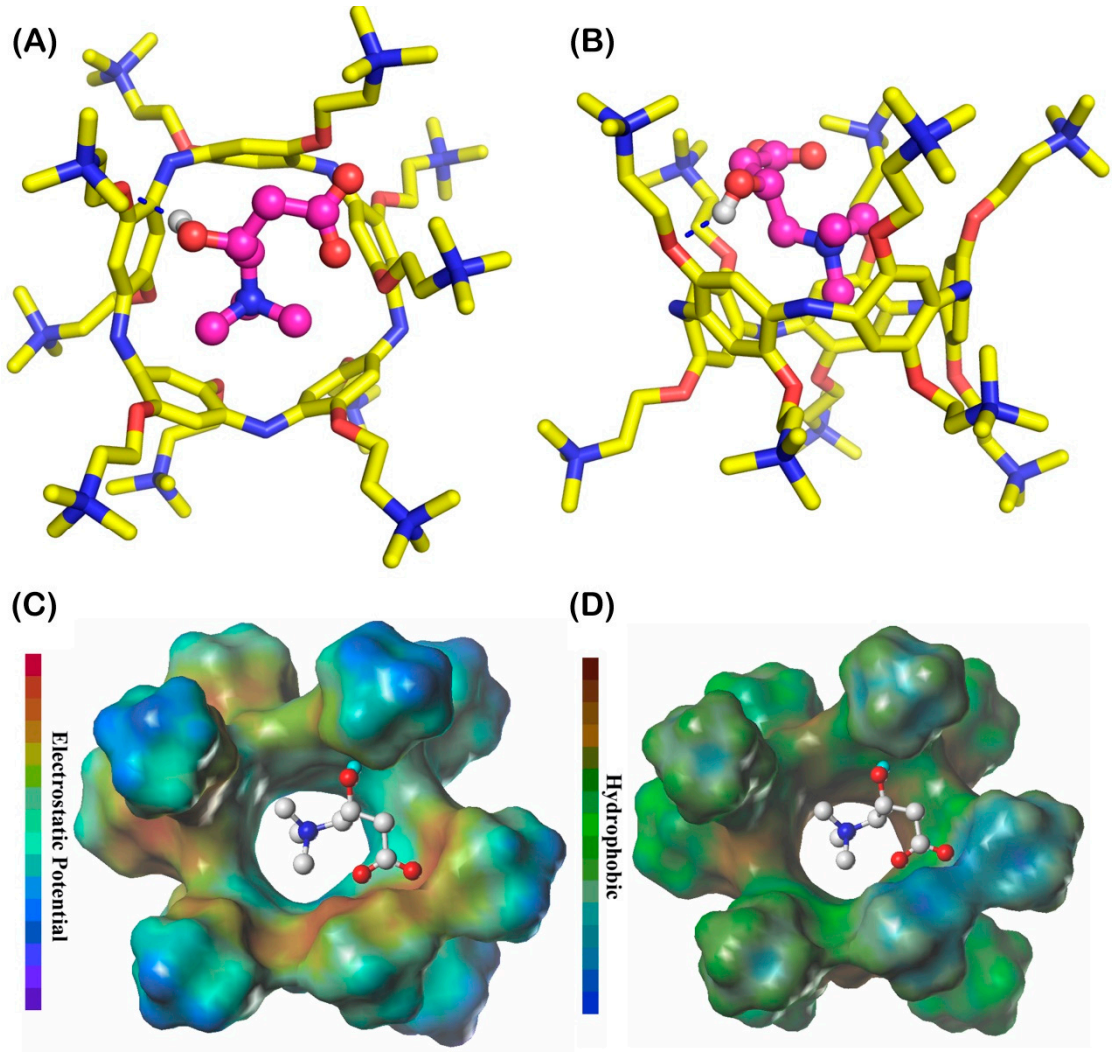

Figure 4. Lowest energy CP5/L-carnitine docked complex for a 1:1 host–guest inclusion (A is the top view, B is the side view); the electrostatic forces (C) (red represents the strongest positive charge, and blue represents the strongest negative charge); the hydrophobic interaction (D) (brown represents the strongest hydrophobic interaction, and blue represents the strongest hydrophilic interaction).

Preprints (www.preprints.org) | NOT PEER-REVIEWED | Posted: 24 October 2018 doi:10.20944/preprints201810.0573.v1

Peer-reviewed version available at Sensors 2018, 18, 3927; doi:10.3390/s18113927

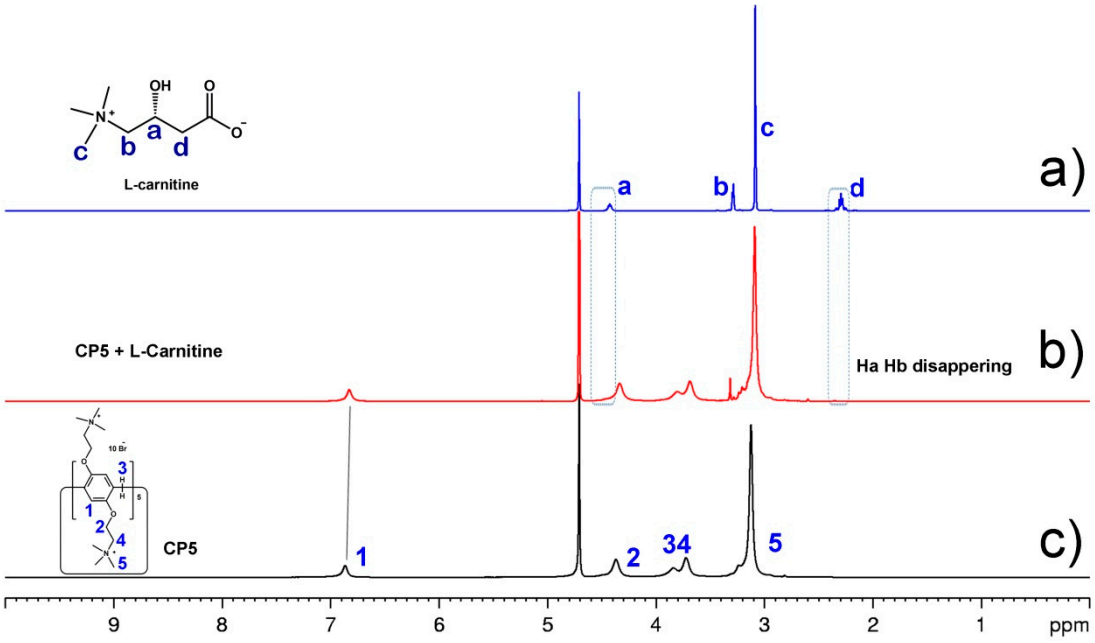

Figure 5. a) ^{1}H NMR spectra (D_2O, 500 MHz, rt) of L-carnitine (10 mM), and b) CP5 + L-carnitine (10 mM) and c) L-carnitine (10 mM), respectively.

3.4. Selectivity and practical samples analysis

The interference study for detection of L-carnitine with the R123B-bound CP5-Gra was measured with 100-fold concentrations of L-carnitine analogues (DA, UA, and AA), the structures of these interferences are shown in **Fig. S10**. Besides, the interferences with common interferences (100-fold concentration) including NaCl, KCl, $MgSO_4$, glucose, sucrose, BSA and tween 20 are also tested. **Fig. 6A** shows that the fluorescence intensity did not change when these interferences were added to R123@CP5@Au-NPs by comparing L-carnitine in the presence of R123@CP5@Au-NPs. **Fig. 6B** shows a significant fluorescence increase upon the addition of L-carnitine. However, the addition of other competitive interferences did not cause significant fluorescence changes, this demonstrates that these interferences did not cause a false-positive signal. To assess the R123@CP5@Au-NPs in practical applications, L-carnitine was detected with a standard addition method in human serum and milk samples (**Table 1**). The recoveries are 93.5–101.7 %, the RSDs are 1.6–4.1 % were obtained by this method. The accuracy and precision of this proposed

Preprints (www.preprints.org) | NOT PEER-REVIEWED | Posted: 24 October 2018 doi:10.20944/preprints201810.0573.v1

Peer-reviewed version available at Sensors 2018, 18, 3927; doi:10.3390/s18113927

approach were satisfactory, which indicated that the proposed method could be applied for the determination of L-carnitine in serum and milk samples.

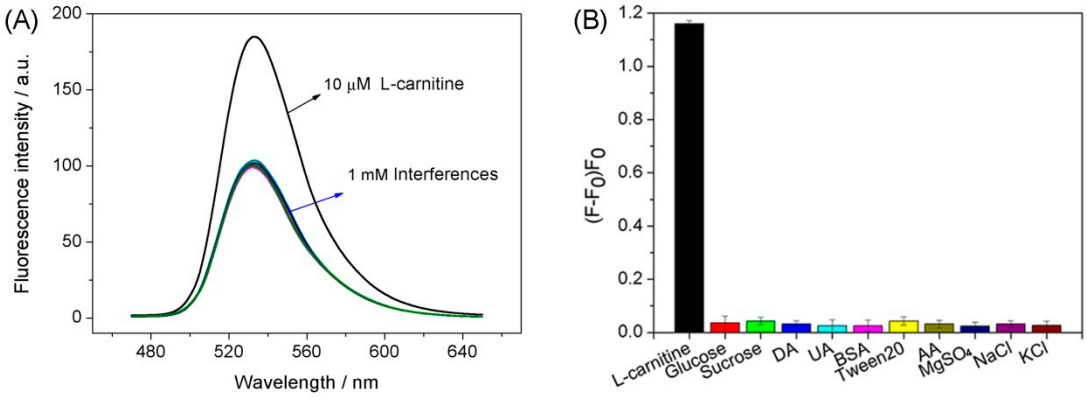

Figure 6. Fluorescent spectra of R123@CP5@Au-NPs in the presence of L-carnitine and others interferences (B). The relative fluorescence intensity of $(F-F_0)/F_0$, and the F_0 and F are the fluorescence intensity without and with the presence of 10 μM L-carnitine and 1 mM interferences (C). The relative fluorescence intensity $[(F-F_0)/F_0]$ of 10 μM L-carnitine in the absence 0.1 mM others interferences (D).

Table 1 Determination of the L-carnitine in human serum and milk samples

Sample	Added (μM)	Founded (μM)	RSD (%)	Recovery (%)
serum	0	0.00		
	2	1.87 ± 0.04	2.1	93.5
	4	4.07 ± 0.17	4.1	101.7
	6	5.82 ± 0.22	3.8	97.0
milk	0	0.00		
	2	1.91 ± 0.03	1.6	95.5
	4	3.97 ± 0.13	3.3	99.2
	6	6.02 ± 0.24	3.9	100.3

4. Conclusions

In summary, we describe a simple and convenient “turn-off-on” fluorescent

sensing platform using cationic water-soluble pillar[5]arene modified Au-NPs and dye Rhodamine 123 as the energy donor-acceptor pair. The outstanding host–guest recognition capability of CP5 and excellent quenching performance of Au-NPs made this sensing system suitable for L-carnitine detection in human serum and milk samples. This work demonstrates that the CP5@Au-NPs composite is a good energy acceptor for fluorescence sensing platforms with potential applications in many fields.

Supporting Information

Synthesis and characterization of CP5 host molecule; the structures of L-carnitine and other interference molecules; the comparison of some reported methods with the present fluorescence approach for determination of L-carnitine; and others information.

Acknowledgements

This work was financially supported by the Program for Leading Talents, the Basic Research Project of Science and Technology Commission of Chongqing (Grant No. cstc2017jcyjAX0031), the Education Commission of Chongqing (Grant No. KJ1712298), and School Enterprise Innovation Platform (Grant No. FLKW2017AAA1024).

References

1. Siwy, Z.; Trofin, L.; Kohli, P.; Baker, L.A.; Protein Biosensors Based on Biofunctionalized Conical Gold Nanotubes. *J. Am. Chem. Soc*. **2005**, *127* 5000−5001.
2. Alvarez-Puebla, R.A.; Liz-Marzan, L.M. Nachweis kleiner anorganischer Moleküle durch oberflächenverstärkte Raman-Streuung, *Angew. Chem*. **2012**, *124*, 11376-11385.
3. Chen, M.S.; Goodman,D.W. Catalytically active gold on ordered titania supports. *Chem. Soc. Rev*. **2008**, *37*, 1860−1870.

4. Hassenkam,T.; Moth-Poulsen, K.; Stuhr-Hansen, N.; Nørgaard, K.; Kabir, M.S.; Bjørnholm, T. Self-Assembly and Conductive Properties of Molecularly Linked Gold Nanowires. *Nano Lett*. **2004**, *4*, 19−22.
5. Zheng, Y.B.; Kiraly, B.; Cheunkar, S.; Huang, T.J.; Weiss, P.S. Incident-Angle-Modulated Molecular Plasmonic Switches: A Case of Weak Exciton-Plasmon Coupling. *Nano Lett*. **2011**, *11*, 2061−2065.
6. Ofir, Y.; Samanta, B.; Rotello, V.M.; Polymer and biopolymer mediated self-assembly of gold nanoparticles, *Chem. Soc. Rev*. **2008**, *37*, 1814−1825.
7. Klajn, R.; Stoddart, J.F.; Grzybowski, B.A. Nanoparticles functionalised with reversible molecular and supramolecular switches. *Chem. Soc. Rev*. **2010**, *39*, 2203−2237.
8. Dalgarno, S.J.; Thallapally, P.K.; Barbour, L.J.; Atwood, J.L. Engineering void space in organic van der Waals crystals: calixarenes lead the way. *Chem. Soc. Rev*. **2007**, *36*, 236–245.
9. Gong, H.-Y.; Rambo, B.M.; Karnas, E.; Lynch, V.M.; Sessler, J.L. A 'Texas-sized' molecular box that forms an anion-induced supramolecular necklace. *Nat. Chem*. **2010**, *2*, 406–409.
10. Ma, X.; Zhao, Y. Biomedical Applications of Supramolecular Systems Based on Host–Guest Interactions. *Chem. Rev*. **2015**, *115*, 7794–7839.
11. Crini, G. Review: A History of Cyclodextrins, *Chem. Rev.* **2014**, *114*, 10940–10975.
12. Cragg, P.; Sharma, J. K. Pillar[5]arenes: fascinating cyclophanes with a bright future. *Chem. Soc. Rev*. **2012**, *41*, 597–607.
13. Ogoshi, T.; Kanai, S.; Fujinami, S.; Yamagishi, T.; Nakamoto, Y. para-Bridged Symmetrical Pillar[5]arenes: Their Lewis Acid Catalyzed Synthesis and Host–Guest Property. *J. Am. Chem. Soc*. **2008**, *130*, 5022–5023.
14. Ogoshi, T.; Yamagishi, T.; Nakamoto, Y. Pillar-Shaped Macrocyclic Hosts Pillar[n]arenes: New Key Players for Supramolecular Chemistry. *Chem. Rev*. **2016**, *116*, 7937–8002.
15. Strutt, N. L.; Zhang, H.C.; Schneebeli, S.T.; Stoddart, J.F. Functionalizing Pillar[n]arenes. *Acc. Chem. Res*. **2014**, *47*, 2631−2642.
16. Xue, M.; Yang, Y.; Chi, X.; Zhang, Z.; Huang, F. Pillararenes, A New Class of Macrocycles for Supramolecular Chemistry. *Acc. Chem. Res*. **2012**, *45*, 1294–1308.

17. Cragg, P. J.; Sharma, K. Pillar[5]arenes: fascinating cyclophanes with a bright future. *Chem. Soc. Rev*. 2012, 41, 597–607.
18. Wei, P.; Yan, X.; Huang, F.H. "Supramolecular polymers constructed by orthogonal self-assembly based on host-guest and metal-ligand interactions". *Chem. Soc. Rev*. **2015**, *44*, 815-832.
19. Wang, K.; Yang, Y.-W.; Zhang, S. X.-A. Progress on the Synthesis and Host-Guest Chemistry of Pillararenes. *Chem. J. Chin. Univ*. **2012**, *33*, 1−13.
20. Wang, K.; Tan, L.-L.; Chen, D.-X.; Song, N.; Xi, G.; Zhang, S. X.-A.; Li, C.; Yang, Y.-W. One-pot synthesis of pillar[n]arenes catalyzed by a minimum amount of TfOH and a solution-phase mechanistic study. *Org. Biomol. Chem*. **2012**, *10*, 9405−9409.
21. Montes-Garcia, V.; Perez-Juste, J.; Pastoriza-Santos, I.; Liz-Marzan, L.M. Metal Nanoparticles and Supramolecular Macrocycles: A Tale of Synergy. *Chem. Eur. J*. 2014, 20, 10874 -10883.
22. Yao, Y.; Xue, M.; Chi, X.D.; Ma, Y.J.; He, J.M.; Abliz, Z.; Huang, F.H. A new water-soluble pillar[5]arene: synthesis and application in the preparation of gold nanoparticles. *Chem. Commun*. **2012**, *48*, 6505−6507.
23. Ji, X. H.; Song, X.N.; Bai, Y.B.; Yang, W.S.; Peng, X.G. Size Control of Gold Nanocrystals in Citrate Reduction: The Third Role of Citrate, *J. Am. Chem. Soc*. **2007**, *129*, 13939−13948.
24. Rowe, M.P.; Plass, K.E.; Kim, K.; Kurdak, Ç.; Zellers, E.T.; Matzger, A.J. Single-Phase Synthesis of Functionalized Gold Nanoparticles. *Chem. Mater*. **2004**, *16*, 3513−3517.
25. Zheng, Y.B.; Payton, J.L.; Song, T.-B.; Pathem, B.K.; Zhao, Y.; Ma, H.; Yang, Y.; Jensen, L.; Jen, A. K.-Y.; Weiss, P.S. Surface-enhanced raman spectroscopy to probe photoreaction pathways and kinetics of isolated reactants on surfaces: flat versus curved substrates. *Nano Lett*. **2012**, *12*, 5362−5368.
26. Li, H.; Chen, D.X.; Sun, Y.L.; Zheng, Y.B.; Tan, L.L.; Weiss, P.S.; Yang, Y.W. Viologen-Mediated Assembly of and Sensing with arboxylatopillar[5]arene-Modified Gold Nanoparticles. *J. Am. Chem. Soc*. **2013**, *135*, 1570−1576.
27. Yao, Y.; Xue, M.; Zhang, Z.B.; Zhang, M.M.; Wang, Y.; Huang, F.H. Gold nanoparticles stabilized by an amphiphilic pillar[5]arene: preparation, self-assembly into composite microtubes in water and application in green catalysis. *Chem. Sci*. **2013**, *4*, 3667–3672.

28 Montes-Garcia, V.; Fernandez-Lopez, C.; Gomez, B.; Perez-Juste, I.; Garcia-Rio, L.; Liz-Marzan, L.M.; Perez-Juste, J.; Pastoriza-Santos, I. Pillar[5]arene-mediated synthesis of gold nanoparticles: size control and sensing capabilities. *Chem. Eur. J.* **2014**, *20*, 8404-8409.

29. Zhao, G.F.; Ran, X.; Zhou, X.; Tan, X.P.; Lei, H.; Xie, X.G.; Yang, L.; Du, G.B. Green synthesis of hydroxylatopillar[5]arene-modified gold nanoparticles and their self-assembly, sensing, and catalysis application. *ACS Sustainable Chem*. Eng. **2018**, *6*, 3938−3947.

30. Seline, K.G.; Johein, H. The determination of L-carnitine in several food samples. *Food Chem*. **2007**, *105*, 793–804.

31. Cao, Q.R.; Ren, S.; Park, M.J.; Choi, Y.J.; Lee, B.J. Determination of highly soluble L-carnitine in biological samples by reverse phase high performance liquid chromatography with fluorescent derivatization. *Arch Pharm Res*. **2007**, *30*, 1041-1046.

32. Wei, D.; Wang, X.; Wang, N.N.; Zhu, Y. A rapid ion chromatography column-switching method for online sample pretreatment and determination of L-carnitine, choline and mineral ions in milk and powdered infant formula. *RSC Adv*. **2017**, *7*, 5920–5927.

33. Kiessig, S.; Vogt, C. Separation of carnitine and acylcarnitines by capillary electrophoresis, *J Chromatogr A* **1997**, 781, 475–479.

34. Kong, Y.; Yang, G.F.; Chen, S.M.; Hou, Z.W.; Du, X.M.; Li, H.; Kong, L.H. Rapid and sensitive determination of L-carnitine and acetyl-L-carnitine in liquid milk samples with capillary zone electrophoresis using indirect UV detection. *Food Anal. Methods* **2018**, *11*, 170–177.

35 Vais, R.D.; Yadegari, H.; Sattarahmady, N.; Helia, H. An anodized nanostructure of Ni/Cu alloy synthesized in ethaline for electrocatalytic oxidation and amperometric determination of L-carnitine. *J Electroanal Chem*. **2018**, *815*, 134–142.

36. Li, H.B.; Zhang, Y.; Wang, X.Q. L-Carnitine capped quantum dots as luminescent probes for cadmium ions. *Sensors and Actuators B* **2007**, *127*, 593–597.

37. Wang, M.H.; Du, J.A.; Mani, V.; Wu, Y.C.; Lin, Y.J.; Chia, Y.M.; Huang, S.T. A rapid fluorescence detecting platform: applicable to sense carnitine and chloramphenicol in food samples. *RSC Adv*. **2014**, *4*, 64112–64118.

38. Mao, X.W.; Tian, D.M.; Li, H.B. p-Sulfonated calix[6]arene modified graphene as

a ‘turn on’ fluorescent probe for L-carnitine in living cellsw. *Chem. Commun*. **2012**, *48*, 4851–4853.

39. Xu, S.F.; Lu, H.Z. Ratiometric fluorescence and mesoporous structure dual signal amplification for sensitive and selective detection of TNT based on MIP@QD fluorescence sensors. *Chem. Commun*. 2015, 51, 3200–3203.
40. Joseph,R.; Naugolny, A.; Feldman, M.; Herzog, I. M.; Fridman, M.; Cohen, Y. Cationic pillararenes potently inhibit biofilm formation without affecting bacterial growth and viability. *J. Am. Chem. Soc*. **2016**, *138*, 754–757.
41. Ma, Y.J.; Ji, X.F.; Xiang, F.; Chi, X.D.; Han, C.Y.; He, J.M.; Abliz, Z.; Chen, W. X.; Huang, F.H. A cationic water-soluble pillar[5]arene: synthesis and host–guest complexation with sodium 1-octanesulfonate. *Chem. Commun*. **2011**, *47*, 12340–12342.
42. Pande, S.; Ghosh, S.K.; Praharaj, S.; Panigrahi, S.; Basu, S.; Jana, S.; Pal, A.; Tsukuda, T.; Pal, T. Synthesis of normal and inverted gold-silver core-shell architectures in β-cyclodextrin and their applications in SERS. *J. Phys. Chem. C* **2007**, *111*, 10806–10813.
43. Kong, B.S.; Geng, J.; Jung, H.T. Layer-by-layer assembly of graphene and gold nanoparticles by vacuum filtration and spontaneous reduction of gold ions. *Chem. Commun*. **2009**, *0*, 2174–2176.
44. Shan, C.; Yang, H.; Han, D.; Zhang, Q.; Ivaska, A.; Niu, L. Graphene/AuNPs/ chitosan nanocomposites film for glucose biosensing. Biosens. Bioelectron **2010**, *25*, 1070–1074.
45. Zhao, Y.; Huang,Y.C.; Zhu, H.; Zhu, Q.Q.; Xia, Y.S. Three-in-one: sensing, self-assembly, and cascade catalysis of cyclodextrin modified gold nanoparticles. *J. Am. Chem. Soc*. **2016**, *138*, 16645−16654.
46. Zhang, N.; Liu, Y.; Tong, L.; Xu, K.; Zhuo, L.; Tang, B. A novel assembly of Au NPs–β-CDs–FL for the fluorescent probing of cholesterol and its application in blood serum. Analyst **2008**, *133*, 1176−1181.
47. Mondal, A.; Jana, N.R. Fluorescent detection of cholesterol using β-cyclodextrin functionalized grapheme. *Chem. Commun*. **2012**, *48*, 7316−7318.
48. Morris, G.M.; Huey, R.; Lindstrom, W., Sanner, M.F.; Takada, Y.; Olson, A.J. AutoDock4 and AutoDockTools4: Automated docking with selective receptor flexibility. *J. Comput. Chem*. **2009**, *30*, 2785–2791.

49. Ogoshi, T.; Takashima, S.; Yamagishi, T. A. Molecular recognition with microporous multi-layer films prepared by layer-by-layer assembly of pillar[5]arenes. *J. Am. Chem. Soc*. **2015**, *137*, 10962−10964.
50. Ogoshi, T.; Yamagishi, T. A.; Nakamoto, Y. Pillar-shaped macrocyclic hosts pillar[n]arenes: new key players for supramolecular chemistry. *Chem. Rev*. **2016**, *116*, 7937–8002.
51. Yao, Y.; Xue, M.; Chen, J.; Zhang, M.; Huang, F. An amphiphilic pillar[5]arene: synthesis, controllable self-assembly in water, and application in calcein release and TNT adsorption. *J. Am. Chem. Soc*. **2012**, *134*, 15712−15715.